

1 SARS-CoV-2 mRNA Vaccine Development Enabled by Prototype Pathogen Preparedness

2

3 Kizzmekia S. Corbett<sup>1#</sup>, Darin Edwards<sup>2#</sup>, Sarah R. Leist<sup>3#</sup>, Olubukola M. Abiona<sup>1</sup>, Seyhan  
4 Boyoglu-Barnum<sup>1</sup>, Rebecca A. Gillespie<sup>1</sup>, Sunny Himansu<sup>2</sup>, Alexandra Schäfer<sup>3</sup>, Cynthia T.  
5 Ziwawo<sup>1</sup>, Anthony T. DiPiazza<sup>1</sup>, Kenneth H. Dinnon<sup>3</sup>, Sayda M. Elbashir<sup>2</sup>, Christine A. Shaw<sup>2</sup>,  
6 Angela Woods<sup>2</sup>, Ethan J. Fritch<sup>4</sup>, David R. Martinez<sup>3</sup>, Kevin W. Bock<sup>5</sup>, Mahnaz Minai<sup>5</sup>, Bianca  
7 M. Nagata<sup>5</sup>, Geoffrey B. Hutchinson<sup>1</sup>, Kapil Bahl<sup>2</sup>, Dario Garcia-Dominguez<sup>2</sup>, LingZhi Ma<sup>2</sup>,  
8 Isabella Renzi<sup>2</sup>, Wing-Pui Kong<sup>1</sup>, Stephen D. Schmidt<sup>1</sup>, Lingshu Wang<sup>1</sup>, Yi Zhang<sup>1</sup>, Laura J.  
9 Stevens<sup>6</sup>, Emily Phung<sup>7</sup>, Lauren A. Chang<sup>1</sup>, Rebecca J. Loomis<sup>1</sup>, Nedim Emil Altaras<sup>2</sup>, Elisabeth  
10 Narayanan<sup>2</sup>, Mihir Metkar<sup>2</sup>, Vlad Presnyak<sup>2</sup>, Catherine Liu<sup>1</sup>, Mark K. Louder<sup>1</sup>, Wei Shi<sup>1</sup>,  
11 Kwanyee Leung<sup>1</sup>, Eun Sung Yang<sup>1</sup>, Ande West<sup>3</sup>, Kendra L. Gully<sup>3</sup>, Nianshuang Wang<sup>8</sup>, Daniel  
12 Wrapp<sup>8</sup>, Nicole A. Doria-Rose<sup>1</sup>, Guillaume Stewart-Jones<sup>2</sup>, Hamilton Bennett<sup>2</sup>, Martha C.  
13 Nason<sup>9</sup>, Tracy J. Ruckwardt<sup>1</sup>, Jason S. McLellan<sup>8</sup>, Mark R. Denison<sup>6</sup>, James D. Chappell<sup>6</sup>, Ian  
14 N. Moore<sup>5</sup>, Kaitlyn M. Morabito<sup>1</sup>, John R. Mascola<sup>1</sup>, Ralph S. Baric<sup>3,4</sup>, Andrea Carfi<sup>2\*</sup>, Barney S.  
15 Graham<sup>1\*</sup>

16

17 #Authors have equal contribution to this study

18

19 <sup>1</sup>Vaccine Research Center; National Institute of Allergy and Infectious Diseases; National  
20 Institutes of Health; Bethesda, Maryland, 20892; United States of America

21 <sup>2</sup>Moderna Inc., Cambridge, MA, 02139; United States of America

22 <sup>3</sup>Department of Epidemiology; University of North Carolina at Chapel Hill; Chapel Hill, North  
23 Carolina, 27599; United States of America

24 <sup>4</sup>Department of Microbiology and Immunology, School of Medicine, University of North Carolina  
25 at Chapel Hill; Chapel Hill, North Carolina, 27599; United States of America

26 <sup>5</sup>National Institute of Allergy and Infectious Diseases; National Institutes of Health; Bethesda,  
27 Maryland, 20892; United States of America

28 <sup>6</sup>Department of Pediatrics, Vanderbilt University Medical Center, Nashville, Tennessee, 37212;  
29 United States of America

30 <sup>7</sup>Institute for Biomedical Sciences, George Washington University, Washington, DC 20052,  
31 United States of America

32 <sup>8</sup>Department of Molecular Biosciences; University of Texas at Austin; Austin, Texas, 78712;  
33 United States of America

34 <sup>9</sup>Biostatistics Research Branch, Division of Clinical Research, National Institute of Allergy and  
35 Infectious Diseases, National Institutes of Health; Bethesda, Maryland, 20892; United States of  
36 America

37

38 \*Correspondence: [bgraham@nih.gov](mailto:bgraham@nih.gov); [Andrea.Carfi@modernatx.com](mailto:Andrea.Carfi@modernatx.com)

39 **Summary**

40 A SARS-CoV-2 vaccine is needed to control the global COVID-19 public health crisis. Atomic-  
41 level structures directed the application of prefusion-stabilizing mutations that improved  
42 expression and immunogenicity of betacoronavirus spike proteins. Using this established  
43 immunogen design, the release of SARS-CoV-2 sequences triggered immediate rapid  
44 manufacturing of an mRNA vaccine expressing the prefusion-stabilized SARS-CoV-2 spike  
45 trimer (mRNA-1273). Here, we show that mRNA-1273 induces both potent neutralizing antibody  
46 and CD8 T cell responses and protects against SARS-CoV-2 infection in lungs and noses of  
47 mice without evidence of immunopathology. mRNA-1273 is currently in a Phase 2 clinical trial  
48 with a trajectory towards Phase 3 efficacy evaluation.

49 Since its emergence in December 2019, severe acute respiratory syndrome coronavirus 2  
50 (SARS-CoV-2) has accounted for over 7 million cases of Coronavirus Disease 2019 (COVID-  
51 19) worldwide in less than 7 months<sup>1</sup>. SARS-CoV-2 is the third novel betacoronavirus in the last  
52 20 years to cause substantial human disease; however, unlike its predecessors SARS-CoV and  
53 MERS-CoV, SARS-CoV-2 transmits efficiently from person-to-person. In absence of a vaccine,  
54 public health measures such as quarantining newly diagnosed cases, contact tracing, and  
55 mandating face masks and physical distancing have been instated to reduce transmission<sup>2</sup>. It is  
56 estimated that until 60-70% population immunity is established, it is unlikely for COVID-19 to be  
57 controlled well enough to resume normal activities. If immunity remains solely dependent on  
58 infection, even at a 1% mortality rate, >40 million people could succumb to COVID-19 globally<sup>3</sup>.  
59 Therefore, rapid development of vaccines against SARS-CoV-2 is critical for changing the  
60 global dynamic of this virus.

61 The spike (S) protein, a class I fusion glycoprotein analogous to influenza hemagglutinin (HA),  
62 respiratory syncytial virus (RSV) fusion glycoprotein (F), and human immunodeficiency virus  
63 (HIV) gp160 (Env), is the major surface protein on the CoV virion and the primary target for  
64 neutralizing antibodies. S proteins undergo dramatic structural rearrangement to fuse virus and  
65 host cell membranes, allowing delivery of the viral genome into target cells. We previously  
66 showed that prefusion-stabilized protein immunogens that preserve neutralization-sensitive  
67 epitopes are an effective vaccine strategy for enveloped viruses, such as RSV<sup>4-8</sup>. Subsequently,  
68 we identified 2 proline substitutions (2P) at the apex of the central helix and heptad repeat 1 that  
69 effectively stabilized MERS-CoV, SARS-CoV and HCoV-HKU1 S proteins in the prefusion  
70 conformation<sup>9-11</sup>. Similar to other prefusion-stabilized fusion proteins, MERS S-2P protein is  
71 more immunogenic at lower doses than wild-type S protein<sup>11</sup>. The 2P has been widely  
72 transferrable to other beta-CoV spike proteins, suggesting a generalizable approach for

73 designing stabilized prefusion beta-CoV S vaccine antigens. This is fundamental to the  
74 prototype pathogen approach for pandemic preparedness<sup>12,13</sup>.

75 Coronaviruses have long been predicted to have a high likelihood of spill over into humans and  
76 cause future pandemics<sup>14,15</sup>. As part of our pandemic preparedness efforts, we have studied  
77 MERS-CoV as prototype pathogen for betacoronaviruses to optimize vaccine design, to dissect  
78 the humoral immune response to vaccination, and identify mechanisms and correlates of  
79 protection. Achieving an effective and rapid vaccine response to a newly emerging virus  
80 requires the precision afforded by structure-based antigen design but also a manufacturing  
81 platform to shorten time to product availability. Producing cell lines and clinical grade subunit  
82 protein typically takes more than 1 year, while manufacturing nucleic acid vaccines can be done  
83 in a matter of weeks<sup>16,17</sup>. In addition to advantages in manufacturing speed, mRNA vaccines are  
84 potentially immunogenic and elicit both humoral and cellular immunity<sup>18-20</sup>. Therefore, we  
85 evaluated mRNA formulated in lipid nanoparticles (mRNA/LNP) as a delivery vehicle for the  
86 MERS S-2P and found that transmembrane-anchored MERS S-2P mRNA elicited better  
87 neutralizing antibody responses than secreted MERS S-2P (**Extended Data Fig. 1a**).

88 Additionally, consistent with protein immunogens, MERS S-2P mRNA was more immunogenic  
89 than MERS wild-type S mRNA (**Extended Data Fig. 1b**). Immunization with MERS S-2P  
90 mRNA/LNP elicited potent neutralizing activity down to a 0.1 µg dose and protected hDPP4  
91 transgenic (288/330<sup>+/+21</sup>) mice against lethal MERS-CoV challenge in a dose-dependent  
92 manner, establishing proof-of-concept that mRNA expressing the stabilized S-2P protein is  
93 protective. Notably, the sub-protective 0.01 µg dose of MERS S-2P mRNA did not cause  
94 exaggerated disease following MERS-CoV infection, but instead resulted in partial protection  
95 against weight loss followed by full recovery without evidence of enhanced illness (**Fig. 1**).

96 In early January 2020, a novel CoV (nCoV) was identified as the cause of a respiratory virus  
97 outbreak occurring in Wuhan, China. Within 24 hours of the release of the SARS-CoV-2 isolate

98 sequences (then known as “2019-nCoV”) on January 10<sup>th</sup>, the 2P mutations were substituted  
99 into S positions aa986 and 987 to produce prefusion-stabilized SARS-CoV-2 S (S-2P) protein  
100 for structural analysis<sup>22</sup> and serological assay development<sup>23,24</sup> *in silico* without additional  
101 experimental validation. Within 5 days of sequence release, current Good Manufacturing  
102 Practice (cGMP) production of mRNA/LNP expressing the SARS-CoV-2 S-2P as a  
103 transmembrane-anchored protein with the native furin cleavage site (mRNA-1273) was initiated  
104 in parallel with preclinical evaluation. Remarkably, this led to the start of a first in human Phase  
105 1 clinical trial on March 16, 2020, 66 days after the viral sequence was released, and a Phase 2  
106 began 74 days later on May 29, 2020 (**Extended Data Fig. 2**). Prior to vaccination of the first  
107 human subject, expression and antigenicity of the S-2P antigen delivered by mRNA was  
108 confirmed *in vitro* (**Extended Data Fig. 3**), and immunogenicity of mRNA-1273 was  
109 documented in several mouse strains. The results of those studies are detailed hereafter.

110 Immunogenicity was assessed in six-week old female BALB/cJ, C57BL/6J, and B6C3F1/J mice  
111 by immunizing intramuscularly (IM) twice with 0.01, 0.1, or 1 µg of mRNA-1273 at a 3-week  
112 interval. mRNA-1273 induced dose-dependent S-specific binding antibodies after prime and  
113 boost in all mouse strains (**Fig. 2a-c**). Potent neutralizing activity was elicited by 1 µg of mRNA-  
114 1273, reaching 819, 89, and 1115 reciprocal IC<sub>50</sub> geometric mean titer (GMT) for BALB/cJ,  
115 C57BL/6J, and B6C3F1/J mice, respectively (**Fig. 2d-f**). These levels are similar to the  
116 neutralization activity achieved by immunizing with 1 µg of SAS-adjuvanted S-2P protein  
117 (**Extended Data Table 1**). To further gauge immunogenicity across a wide dose range,  
118 BALB/cJ mice were immunized with 0.0025 – 20 µg of mRNA-1273 revealing a strong positive  
119 correlation between dose-dependent mRNA-1273-elicited binding and neutralizing antibody  
120 responses (**Extended Data Fig. 4**). BALB/cJ mice that received a single dose of mRNA-1273  
121 were evaluated in order to ascertain the utility for a one-dose vaccine regimen. S-binding  
122 antibodies were induced in mice immunized with one dose of 1 or 10 µg of mRNA-1273, and the

123 10 µg dose elicited neutralizing antibody activity that increased between week 2 and week 4,  
124 reaching 315 reciprocal IC<sub>50</sub> GMT (**Extended Data Fig. 5a-b**). These data demonstrate that  
125 mRNA expressing SARS-CoV-2 S-2P is a potent immunogen and neutralizing activity can be  
126 elicited with a single dose.

127 Next, we evaluated the balance of Th1 and Th2, because vaccine-  
128 associated enhanced respiratory disease (VAERD) has been associated with Th2-biased  
129 immune responses in children immunized with whole-inactivated virus vaccines against RSV  
130 and measles virus<sup>25,26</sup>. A similar phenomenon has also been reported in some animal models  
131 with whole-inactivated SARS-CoV vaccines<sup>27</sup>. Thus, we first compared levels of S-specific  
132 IgG2a/c and IgG1, which are surrogates of Th1 and Th2 responses respectively, elicited by  
133 mRNA-1273 to those elicited by SARS-CoV-2 S-2P protein adjuvanted with the TLR4-agonist  
134 Sigma Adjuvant System (SAS). Both immunogens elicited IgG2a and IgG1 subclass S-binding  
135 antibodies, indicating a balanced Th1/Th2 response (**Fig. 3a-c; Extended Data Fig. 6**). The S-  
136 specific IgG subclass profile following a single dose of mRNA-1273 (**Extended Data Fig. 5c**)  
137 was similar to that observed following two doses. In contrast, Th2-biased antibodies with lower  
138 IgG2a/IgG1 subclass response ratios were observed in mice immunized with SARS-CoV-2 S  
139 protein formulated in alum (**Extended Data Fig. 7a-b**). Following re-stimulation with peptide  
140 pools (S1 and S2) corresponding to the S protein, splenocytes from mRNA-1273-immunized  
141 mice secreted more IFN-γ than IL-4, IL-5, or IL-13 whereas SARS-CoV-2 S protein with alum  
142 induced Th2-skewed cytokine secretion (**Extended Data Fig. 7c-d**). 7 weeks post-boost, we  
143 also directly measured cytokine patterns in vaccine-induced memory T cells by intracellular  
144 cytokine staining (ICS); mRNA-1273-elicited CD4<sup>+</sup> T cells re-stimulated with S1 or S2 peptide  
145 pools exhibited a Th1-dominant response, particularly at higher immunogen doses (**Fig. 3d-e**).  
146 Furthermore, 1 µg of mRNA-1273 induced a robust CD8<sup>+</sup> T cell response to the S1 peptide pool  
147 (**Fig. 3f-g**). The Ig subclass and T cell cytokine data together demonstrate that immunization

148 with mRNA-1273 elicits a balanced Th1/Th2 response in contrast to the Th2-biased response  
149 seen with S protein adjuvanted with alum, suggesting that mRNA vaccination avoids Th2-biased  
150 immune responses that have been linked to VAERD.

151 Protective immunity was assessed in young adult BALB/cJ mice challenged with mouse-  
152 adapted (MA) SARS-CoV-2 that exhibits viral replication localized to lungs and nasal  
153 turbinates<sup>28</sup>. BALB/cJ mice that received two 1 µg doses of mRNA-1273 were completely  
154 protected from viral replication in lungs after challenge at a 5- (**Fig. 4a**) or 13-week intervals  
155 following boost (**Extended Data Fig. 8a**). mRNA-1273-induced immunity also rendered viral  
156 replication in nasal turbinates undetectable in 6 out of 7 mice (**Fig. 4b, Extended Data Fig. 8b**).  
157 Efficacy of mRNA-1273 was dose-dependent, with two 0.1 µg mRNA-1273 doses reducing lung  
158 viral load by ~100-fold and two 0.01 µg mRNA-1273 doses reducing lung viral load by ~3-fold  
159 (**Fig. 4a**). Of note, mice challenged 7 weeks after a single dose of 1 µg or 10 µg of mRNA-1273  
160 were also completely protected against lung viral replication (**Fig. 4c**). Challenging animals  
161 immunized with sub-protective doses provides an orthogonal assessment of safety signals,  
162 such as increased clinical illness or pathology. Similar to what was observed with MERS-CoV S-  
163 2P mRNA, mice immunized with sub-protective 0.1 and 0.01 µg mRNA-1273 doses showed no  
164 evidence of enhanced lung pathology or excessive mucus production (**Fig. 4d**). In summary,  
165 mRNA-1273 is immunogenic, efficacious, and does not show evidence of promoting VAERD  
166 when given at sub-protective doses in mice.

167 Here, we showed that 1 µg of mRNA-1273 was sufficient to induce robust neutralizing activity  
168 and CD8 T cell responses, balanced Th1/Th2 antibody isotype responses, and protection from  
169 viral replication for more than 3 months following a prime/boost regimen similar to that being  
170 tested in humans. Inclusion of lower sub-protective doses demonstrated the dose-dependence  
171 of antibody, Th1 CD4 T cell responses, and protection, suggesting immune correlates of  
172 protection can be further elucidated. A major goal of animal studies to support SARS-CoV-2



173 vaccine candidates through clinical trials is to not only prove elicitation of potent protective  
174 immune responses, but to show that sub-protective responses do not cause VAERD<sup>3</sup>. Sub-  
175 protective doses did not prime mice for enhanced immunopathology following challenge.  
176 Moreover, the induction of protective immunity following a single dose suggests that  
177 consideration could be given to administering one dose of this vaccine in the outbreak setting.  
178 These data, combined with immunogenicity data from nonhuman primates and subjects in early  
179 Phase 1 clinical trials, will be used to inform the dose and regimen of mRNA-1273 in advanced  
180 clinical efficacy trials.

181 The COVID-19 pandemic of 2020 is the Pathogen X event that has long been predicted<sup>12,13</sup>.  
182 Here, we provide a paradigm for rapid vaccine development. Structure-guided stabilization of  
183 the MERS-CoV S protein combined with a fast, scalable, and safe mRNA/LNP vaccine platform  
184 led to a generalizable beta-CoV vaccine solution that translated into a commercial mRNA  
185 vaccine delivery platform, paving the way for the rapid response to the COVID-19 outbreak. This  
186 is a demonstration of how the power of new technology-driven concepts like synthetic  
187 vaccinology facilitate a vaccine development program that can be initiated with pathogen  
188 sequences alone<sup>11</sup>. It is also a proof-of-concept for the prototype pathogen approach for  
189 pandemic preparedness and response that is predicated on identifying generalizable solutions  
190 for medical countermeasures within virus families or genera<sup>12</sup>. Even though the response to the  
191 COVID-19 pandemic is unprecedented in its speed and breadth, we envision a response that  
192 could be quicker. There are 24 other virus families known to infect humans, and with sustained  
193 investigation of those potential threats, we could be better prepared for future looming  
194 pandemics<sup>13</sup>.

195

196 **Acknowledgements**

197 We thank Gabriela Alvarado, Karin Bok, Kevin Carlton, Masaru Kanekiyo, Robert Seder, and  
198 additional members of all included laboratories for critical discussions, advice, and review of the  
199 manuscript. We thank Judy Stein and Monique Young for technology transfer and administrative  
200 support, respectively. We thank members of the NIH NIAID VRC Translational Research  
201 Program for technical assistance with mouse experiments. This work was supported by the  
202 Intramural Research Program of the VRC and the Division of Intramural Research, NIAID, NIH  
203 (B.S.G) and NIH NIAID grant R01-AI127521 (J.S.M.). mRNA-1273 has been funded in part with  
204 Federal funds from the Department of Health and Human Services, Office of the Assistant  
205 Secretary for Preparedness and Response, Biomedical Advanced Research and Development  
206 Authority, under Contract 75A50120C00034. PRNT assays were funded under NIH Contract  
207 HHSN261200800001E Agreement 17x198 (to J.D.C.), furnished through Leidos Biomedical  
208 Research, Inc. MERS mRNA mouse challenge studies were funded under NIH Contract  
209 HHSN272201700036I Task Rrder No. 75N93019F00132 Requisition No. 5494549 (to R.B.).  
210 K.S.C.'s research fellowship was partially funded by the Undergraduate Scholarship Program,  
211 Office of Intramural Training and Education, Office of the Director, NIH. D.R.M. was funded by  
212 NIH NIAID grant T32-AI007151 and a Burroughs Wellcome Fund Postdoctoral Enrichment  
213 Program Award.

214

## 215 **Author Contributions**

216 K.S.C., D.K.E., S.R.L., O.M.A, S.B.B., R.A.G., S.H., A.S., C.Z., A.T.D., K.H.D., S.E., C.A.S.,  
217 A.W., E.J.F., D.R.M, K.W.B., M.M., B.M.N., G.B.H., K.B., D.G.D., L.M., I.R., W.P.K, S.S., L.W.,  
218 Y.Z., J.C., L.S., L.A.C., E.P., R.J.L., N.E.A., E.N., M.M., V.P., C.L., M.K.L., W.S., K.G., K.L.,  
219 E.S.Y., A.W., G.A., N.A.D.R., G.S.J., H.B., M.N., T.J.R., M.R.D., I.N.M., K.M.M., J.R.M., R.S.B.,  
220 A.C., and B.S.G. designed, completed, and/or analyzed experiments. N.W., D.W., and J.S.M.  
221 contributed new reagents/analytic tools. K.S.C., K.M.M, and B.S.G. wrote the manuscript. All  
222 authors contributed to discussions in regard to and editing of the manuscript.

223

## 224 **Competing Interest Declaration**

225 K.S.C., N.W., J.S.M., and B.S.G. are inventors on International Patent Application No.

226 WO/2018/081318 entitled “Prefusion Coronavirus Spike Proteins and Their Use.” K.S.C., O.M.A.,

227 G.B.H., N.W., D.W., J.S.M, and B.S.G. are inventors on US Patent Application No. 62/972,886

228 entitled “2019-nCoV Vaccine”. R.S.B. filed an invention report for the SARS-CoV-2 MA virus

229 (UNC ref. #18752).

230

## 231 **Additional Information**

232 Correspondence and requests for materials should be addressed to Barney S. Graham,

233 bgraham@nih.gov and Andrea Carfi, andrea.carfi@modernatx.com.

234

## 235 **Methods**

### 236 MERS-CoV S-2P and SARS-CoV-2 S-2P mRNA synthesis and lipid nanoparticle formulation

237 For each vaccine, T7 RNA polymerase-mediated transcription was used *in vitro* to synthesize

238 the mRNA from a linearized DNA template, which flanked the immunogen open-reading frames

239 with the 5' and 3' untranslated regions and a poly-A tail as described previously<sup>29</sup>. mRNA was

240 then purified, diluted in citrate buffer to the desired concentration and encapsulated into lipid

241 nanoparticles (LNP) by ethanol drop nanoprecipitation. At molar ratio of 50:10:38.5:1.5

242 (ionizable lipid:DSPC:cholesterol:PEG-lipid), lipids were dissolved in ethanol and combined with

243 a 6.25-mM sodium acetate buffer (pH 5) containing mRNA at a ratio of 3:1 (aqueous:ethanol).

244 Formulations were dialyzed against phosphate-buffered saline (pH 7.4) for at least 18 hr,

245 concentrated using Amicon ultracentrifugal filters (EMD Millipore), passed through a 0.22- $\mu$ m

246 filter and stored at -20°C until use. All formulations underwent quality control for particle size,

247 RNA encapsulation, and endotoxin. LNP were between 80 – 100 nm in size, with > 90%  
248 encapsulation on mRNA and < 10 EU/mL endotoxin.

#### 249 MERS-CoV and SARS-CoV Protein Expression and Purification

250 Vectors encoding MERS-CoV S-2P<sup>11</sup> and SARS-CoV S-2P<sup>22</sup> were generated as previously  
251 described with the following small amendments. Proteins were expressed by transfection of  
252 plasmids into Expi293 cells using Expifectamine transfection reagent (ThermoFisher) in  
253 suspension at 37°C for 4-5 days. Transfected cell culture supernatants were collected, buffer  
254 exchanged into 1X PBS, and protein was purified using Strep-Tactin resin (IBA). For proteins  
255 used for mouse inoculations, tags were cleaved with addition of HRV3C protease  
256 (ThermoFisher) (1% wt/wt) overnight at 4 °C. Size exclusion chromatography using Superose 6  
257 Increase column (GE Healthcare) yielded final purified protein.

#### 258 Design and Production of Recombinant Minifibrin Foldon Protein

259 A mammalian codon-optimized plasmid encoding foldon inserted minifibrin  
260 (ADIVLNDLPFVDGPPAEGQSRISWIKNGEELGADTQYGSEGSMMNRPTVSVLRNVEVL DKNIGI  
261 LKTSLETANS DIKTIQEAGYIPEAPRDGQAYVRKDG EWVLLSTFLSPALVPRGSHHHHHHSAWS  
262 HPQFEK) with a C-terminal thrombin cleavage site, 6x His-tag, and Strep-TagII was  
263 synthesized and subcloned into a mammalian expression vector derived from pLEXm. The  
264 construct was expressed by transient transfection of Expi293 (ThermoFisher) cells in  
265 suspension at 37°C for 5 days. The protein was first purified with a Ni<sup>2+</sup>-nitrilotriacetic acid (NTA)  
266 resin (GE Healthcare,) using an elution buffer consisting of 50 mM Tris-HCl, pH 7.5, 400 mM  
267 NaCl, and 300 mM imidazole, pH 8.0, followed by purification with StrepTactin resin (IBA)  
268 according to the manufacturer's instructions.

#### 269 Cell Lines

270 HEK293T/17 (ATCC #CRL-11268), Vero E6 (ATCC), Huh7.5 cells (provided by Deborah R.  
271 Taylor, US Food and Drug Administration), and ACE-2-expressing 293T cells (provided by  
272 Michael Farzan, Scripps Research Institute) were cultured in Dulbecco's modified Eagle's  
273 medium (DMEM) supplemented with 10% FBS, 2 mM glutamine, and 1% penicillin/streptomycin  
274 at 37°C and 5% CO<sub>2</sub>. Vero E6 cells used in plaque assays to determine lung and nasal  
275 turbinate viral titers were cultured in DMEM supplemented with 10% Fetal Clone II and 1%  
276 anti/anti at 37C and 5% CO<sub>2</sub>. Vero E6 cells used in PRNT assays were cultured in DMEM  
277 supplemented with 10% Fetal Clone II and amphotericin B [0.25 µg/ml] at 37C and 5% CO<sub>2</sub>.  
278 Expi293 cells were maintained in manufacturer's suggested media.

#### 279 In vitro mRNA Expression

280 HEK293T cells were transiently transfected with mRNA encoding SARS-CoV-2 WT S or S-2P  
281 protein using a TranIT mRNA transfection kit (Mirus). After 24 hr, the cells were harvested and  
282 resuspended in FACS buffer (1X PBS, 3% FBS, 0.05% sodium azide). To detect surface protein  
283 expression, the cells were stained with 10 µg/mL ACE2-FLAG (Sigma) or CR3022<sup>30</sup> in FACS  
284 buffer for 30 min on ice. Thereafter, cells were washed twice in FACS buffer and incubated with  
285 FITC anti-FLAG (Sigma) or Alexafluor 647 goat anti-human IgG (Southern Biotech) in FACS  
286 buffer for 30 min on ice. Live/Dead aqua fixable stain (Invitrogen) were utilized to assess  
287 viability. Data acquisition was performed on a BD LSRII Fortessa instrument (BD Biosciences)  
288 and analyzed by FlowJo software v10 (Tree Star, Inc.)

#### 289 Mouse Models

290 Animal experiments were carried out in compliance with all pertinent US National Institutes of  
291 Health regulations and approval from the Animal Care and Use Committee of the Vaccine  
292 Research Center, Moderna Inc., or University of North Carolina at Chapel Hill. For  
293 immunogenicity studies, 6-8-week-old female BALB/c (Charles River), BALB/cJ, C57BL/6J, or  
294 B6C3F1/J mice (Jackson Laboratory) were used. mRNA formulations were diluted in 50 µL of

295 1X PBS, and mice were inoculated IM into the same hind leg for both prime and boost. For all  
296 SARS-CoV-2 S-P protein vaccinations, mice were inoculated IM, with SAS, as previously  
297 detailed<sup>11</sup>. For S + alum immunizations, SARS-CoV-2 S protein (Sino Biological) + 250 µg alum  
298 hydrogel was delivered IM. For challenge studies to evaluate MERS-CoV-2 vaccines, 16-20-  
299 week-old 288/330<sup>+/+</sup> mice<sup>21</sup> were immunized. Four weeks post-boost, pre-challenge sera were  
300 collected from a subset of mice, and remaining mice were challenged with 5x10<sup>5</sup> PFU of a  
301 mouse-adapted MERS-CoV EMC derivative, m35c4<sup>31</sup>. On day 3 post-challenge, lungs were  
302 harvested, and hemorrhage and viral titer were assessed, per previously published methods<sup>32</sup>.  
303 For challenge studies to evaluate SARS-CoV-2 vaccines, BALB/cJ mice were challenged with  
304 10<sup>5</sup> PFU of mouse-adapted SARS-CoV-2 (SARS-CoV-2 MA). On day 2 post-challenge, lungs  
305 and nasal turbinates were harvested for viral titer assessment, per previously published  
306 methods<sup>28</sup>.

### 307 Histology

308 Lungs from mice were collected at the indicated study endpoints and placed in 10% neutral  
309 buffered formalin (NBF) until adequately fixed. Thereafter, tissues were trimmed to a thickness  
310 of 3-5 mm, processed and paraffin embedded. The respective paraffin tissue blocks  
311 were sectioned at 5 µm and stained with hematoxylin and eosin (H&E). All sections were  
312 examined by a board-certified veterinary pathologist using an Olympus BX51 light microscope  
313 and photomicrographs were taken using an Olympus DP73 camera.

### 314 Enzyme-linked Immunosorbent Assay (ELISA)

315 Nunc Maxisorp ELISA plates (ThermoFisher) were coated with 100 ng/well of protein in 1X PBS  
316 at 4°C for 16 hr. Where applicable, to eliminate fold-on-specific binding from MERS S-2P- or  
317 SARS-CoV-2 S-2P protein-immune mouse serum, 50 µg/mL of fold-on protein was added for 1  
318 hr at room temperature (RT). After standard washes and blocks, plates were incubated with

319 serial dilutions of heat-inactivated (HI) sera for 1 hr at RT. Following washes, anti-mouse IgG,  
320 IgG1, or IgG2a or IgG2c–horseradish peroxidase conjugates (ThermoFisher) were used as  
321 secondary Abs, and 3,5,3'5'-tetramethylbenzidine (TMB) (KPL) was used as the substrate to  
322 detect Ab responses. Endpoint titers were calculated as the dilution that emitted an optical  
323 density exceeding 4X background (secondary Ab alone).

#### 324 Pseudovirus Neutralization Assay

325 We introduced divergent amino acids, as predicted from translated sequences, into the CMV/R-  
326 MERS-CoV EMC S (GenBank#: AFS88936) gene<sup>33</sup> to generate a MERS-CoV m35c4 S gene<sup>31</sup>.  
327 To produce SARS-CoV-2 pseudoviruses, a codon-optimized CMV/R-SARS-CoV-2 S (Wuhan-1,  
328 Genbank #: MN908947.3) plasmid was constructed. Pseudoviruses were produced by co-  
329 transfection of plasmids encoding a luciferase reporter, lentivirus backbone, and S genes into  
330 HEK293T/17 cells (ATCC #CRL-11268), as previously described<sup>33</sup>. For SARS-CoV-2  
331 pseudovirus, human transmembrane protease serine 2 (TMPRSS2) plasmid was also co-  
332 transfected<sup>34</sup>. Pseudoneutralization assay methods have been previously described<sup>11</sup>. Briefly, HI  
333 serum was mixed with pseudoviruses, incubated, and then added to Huh7.5 cells or ACE-2-  
334 expressing 293T cells, for MERS-CoV and SARS-CoV-2 respectively. Seventy-two hr later, cells  
335 were lysed, and luciferase activity (relative light units, RLU) was measured. Percent  
336 neutralization was normalized considering uninfected cells as 100% neutralization and cells  
337 infected with only pseudovirus as 0% neutralization. IC<sub>50</sub> titers were determined using a log  
338 (agonist) vs. normalized response (variable slope) nonlinear function in Prism v8 (GraphPad).

#### 339 Plaque Reduction Neutralization Test (PRNT)

340 HI sera were diluted in gelatin saline (0.3% [wt/vol] gelatin in phosphate-buffered saline  
341 supplemented with CaCl<sub>2</sub> and MgCl<sub>2</sub>) to generate a 1:5 dilution of the original specimen, which  
342 served as a starting concentration for further serial log<sub>4</sub> dilutions terminating in 1:81,920. Sera

343 were combined with an equal volume of SARS-CoV-2 clinical isolate 2019-nCoV/USA-WA1-  
344 F6/2020 in gelatin saline, resulting in an average concentration of 730 plaque-forming units per  
345 mL (determined from plaque counts of 24 individual wells of untreated virus) in each serum  
346 dilution. Thus, final serum concentrations ranged from 1:10 to 1:163,840 of the original.  
347 Virus/serum mixtures were incubated for 20 min at 37 °C, followed by adsorption of 0.1 mL to  
348 each of two confluent Vero E6 cell monolayers (in 10-cm<sup>2</sup> wells) for 30 min at 37°C. Cell  
349 monolayers were overlaid with Dulbecco's modified Eagle's medium (DMEM) containing 1%  
350 agar and incubated for 3 d at 37°C in humidified 5% CO<sub>2</sub>. Plaques were enumerated by direct  
351 visualization. The average number of plaques in virus/serum (duplicate) and virus-only (24)  
352 wells was used to generate percent neutralization curves according the following formula: 1 –  
353 (ratio of mean number of plaques in the presence and absence of serum). The PRNT IC<sub>50</sub> titer  
354 was defined as the reciprocal serum dilution at which the neutralization curve crossed the 50%  
355 threshold.

#### 356 Intracellular Cytokine Staining

357 Mononuclear single cell suspensions from whole mouse spleens were generated using a  
358 gentleMACS tissue dissociator (Miltenyi Biotec) followed by 70 µm filtration and density gradient  
359 centrifugation using Fico/Lite-LM medium (Atlanta Biologicals). Cells from each mouse were  
360 resuspended in R10 media (RPMI 1640 supplemented with Pen-Strep antibiotic, 10% HI-FBS,  
361 Glutamax, and HEPES) and incubated for 6 hr at 37°C with protein transport inhibitor cocktail  
362 (eBioscience) under three conditions: no peptide stimulation, and stimulation with two spike  
363 peptide pools (JPT product PM-WCPV-S-1). Peptide pools were used at a final concentration of  
364 2 µg/mL each peptide. Cells from each group were pooled for stimulation with cell stimulation  
365 cocktail (eBioscience) as a positive control. Following stimulation, cells were washed with PBS  
366 prior to staining with LIVE/DEAD Fixable Blue Dead Cell Stain (Invitrogen) for 20 min at RT.  
367 Cells were then washed in FC buffer (PBS supplemented with 2% HI-FBS and 0.05% NaN<sub>3</sub>)



368 and resuspended in BD Fc Block (clone 2.4G2) for 5 min at RT prior to staining with a surface  
369 stain cocktail containing the following antibodies purchased from BD and Biolegend: I-A/I-E  
370 (M5/114.15.2) PE, CD8a (53-6.7) BUV805, CD44 (IM7) BUV395, CD62L (MEL-14) BV605, and  
371 CD4 (RM4-5) BV480 in brilliant stain buffer (BD). After 15 min, cells were washed with FC buffer  
372 then fixed and permeabilized using the BD Cytofix/Cytoperm fixation/permeabilization solution  
373 kit according to manufacturer instructions. Cells were washed in perm/wash solution and  
374 stained with Fc Block (5 min at RT), followed by intracellular staining (30 min at 4°C) using a  
375 cocktail of the following antibodies purchased from BD, Biolegend, or eBioscience: CD3e (17A2)  
376 BUV737, IFN- $\gamma$  (XMG1.2) BV650, TNF- $\alpha$  (MP6-XT22) BV711, IL-2 (JES6-5H4) BV421, IL-4  
377 (11B11) Alexa Fluor 488, and IL-5 (TRFK5) APC in 1x perm/wash diluted with brilliant stain  
378 buffer. Finally, cells were washed in perm/wash solution and resuspended in 0.5% PFA-FC  
379 stain buffer prior to running on a Symphony A5 flow cytometer (BD). Analysis was performed  
380 using FlowJo software, version 10.6.2 according to the gating strategy outlined in **Extended**  
381 **Data Figure 9**. Background cytokine expression in the no peptide condition was subtracted from  
382 that measured in the S1 and S2 peptide pools for each individual mouse.

### 383 T Cell Stimulation and Cytokine Analysis

384 Spleens from immunized mice were collected 2 weeks post-boost.  $2 \times 10^6$  splenocytes/well (96-  
385 well plate) were stimulated *in vitro* with two peptide libraries, JPT1 and JPT2, (15mers with 11  
386 aa overlap) covering the entire SARS-CoV-2 spike protein (JPT product PM-WCPV-S-1). Both  
387 peptide libraries were used at a final concentration of 1  $\mu\text{g}/\text{mL}$ . After 24 hr of culture at 37°C, the  
388 plates were centrifuged and supernatant was collected and frozen at -80°C for cytokine  
389 detection. Measurements and analyses of secreted cytokines from a murine 35-plex kit were  
390 performed using a multiplex bead-based technology (Luminex) assay with a Bio-Plex 200  
391 instrument (Bio-Rad) after 2-fold dilution of supernatants.

392 Statistical Analysis

393 Geometric means or means are represented by the heights of bars, or symbols, and error bars  
394 represent the corresponding SD. Dotted lines indicate assay limits of detection. Mann-Whitney  
395 tests were used to compare 2 experimental groups and Wilcoxon signed rank tests to compare  
396 the same animals at different time points. To compare >2 experimental groups, Kruskal-Wallis  
397 ANOVA with Dunn's multiple comparisons tests were applied. For antibody responses  
398 in **Extended Data Fig. 4c**, a Spearman correlation test was used to correlate binding antibody  
399 titers to neutralizing antibody titers. \* = p-value < 0.05, \*\* = p-value < 0.01, \*\*\* = p-value < 0.001,  
400 \*\*\*\* = p-value < 0.0001.

## References

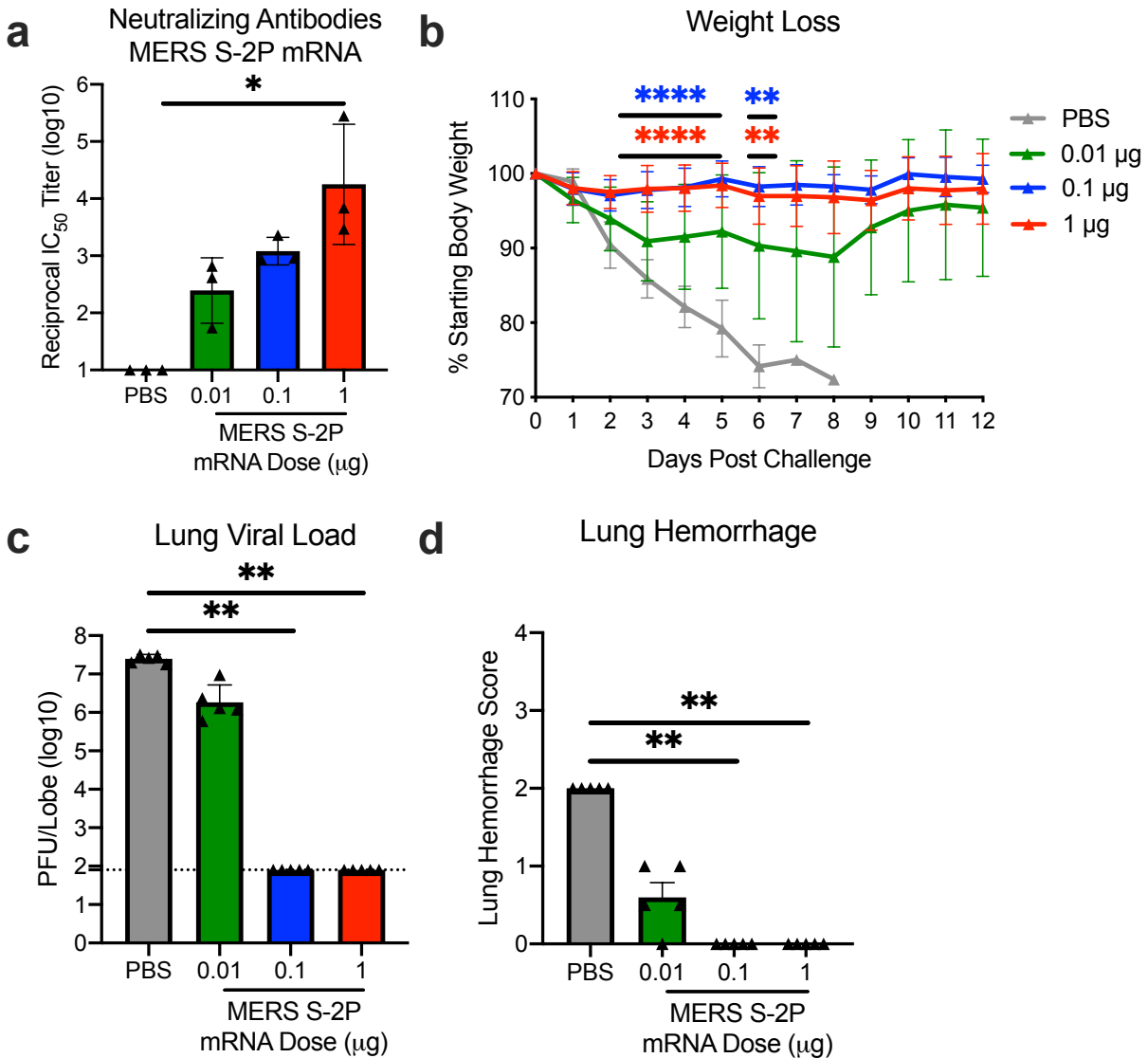
- 401  
402  
403 1 Dong, E., Du, H. & Gardner, L. An interactive web-based dashboard to track COVID-19  
404 in real time. *The Lancet Infectious Diseases* **20**, 533-534,  
405 doi:[https://doi.org/10.1016/S1473-3099\(20\)30120-1](https://doi.org/10.1016/S1473-3099(20)30120-1) (2020).  
406 2 Keni, R., Alexander, A., Nayak, P. G., Mudgal, J. & Nandakumar, K. COVID-19:  
407 Emergence, Spread, Possible Treatments, and Global Burden. *Frontiers in Public Health*  
408 **8**, doi:10.3389/fpubh.2020.00216 (2020).  
409 3 Graham, B. S. Rapid COVID-19 vaccine development. *Science* **368**, 945-946,  
410 doi:10.1126/science.abb8923 (2020).  
411 4 Graham, B. S., Gilman, M. S. A. & McLellan, J. S. Structure-Based Vaccine Antigen  
412 Design. *Annu Rev Med* **70**, 91-104, doi:10.1146/annurev-med-121217-094234 (2019).  
413 5 McLellan, J. S. *et al.* Structure of RSV fusion glycoprotein trimer bound to a prefusion-  
414 specific neutralizing antibody. *Science* **340**, 1113-1117, doi:10.1126/science.1234914  
415 (2013).  
416 6 McLellan, J. S. *et al.* Structure-based design of a fusion glycoprotein vaccine for  
417 respiratory syncytial virus. *Science* **342**, 592-598, doi:10.1126/science.1243283 (2013).  
418 7 Crank, M. C. *et al.* A proof of concept for structure-based vaccine design targeting RSV  
419 in humans. *Science* **365**, 505-509 (2019).  
420 8 Gilman, M. S. A. *et al.* Rapid profiling of RSV antibody repertoires from the memory B  
421 cells of naturally infected adult donors. *Sci Immunol* **1**, doi:10.1126/sciimmunol.aaj1879  
422 (2016).  
423 9 Walls, A. C. *et al.* Cryo-electron microscopy structure of a coronavirus spike glycoprotein  
424 trimer. *Nature* **531**, 114-117, doi:10.1038/nature16988 (2016).  
425 10 Kirchdoerfer, R. N. *et al.* Pre-fusion structure of a human coronavirus spike protein.  
426 *Nature* **531**, 118-121, doi:10.1038/nature17200 (2016).  
427 11 Pallesen, J. *et al.* Immunogenicity and structures of a rationally designed prefusion  
428 MERS-CoV spike antigen. *Proceedings of the National Academy of Sciences* **114**,  
429 E7348-E7357, doi:10.1073/pnas.1707304114 (2017).  
430 12 Graham, B. S. & Sullivan, N. J. Emerging viral diseases from a vaccinology perspective:  
431 preparing for the next pandemic. *Nat Immunol* **19**, 20-28, doi:10.1038/s41590-017-0007-  
432 9 (2018).  
433 13 Graham, B. S. & Corbett, K. S. Prototype pathogen approach for pandemic  
434 preparedness: world on fire. *J Clin Invest*, doi:10.1172/JCI139601 (2020).  
435 14 Menachery, V. D. *et al.* A SARS-like cluster of circulating bat coronaviruses shows  
436 potential for human emergence. *Nat Med* **21**, 1508-1513, doi:10.1038/nm.3985 (2015).  
437 15 Menachery, V. D. *et al.* SARS-like WIV1-CoV poised for human emergence. *Proc Natl*  
438 *Acad Sci U S A* **113**, 3048-3053, doi:10.1073/pnas.1517719113 (2016).  
439 16 Graham, B. S., Mascola, J. R. & Fauci, A. S. Novel Vaccine Technologies: Essential  
440 Components of an Adequate Response to Emerging Viral Diseases. *JAMA* **319**, 1431-  
441 1432, doi:10.1001/jama.2018.0345 (2018).  
442 17 Dowd, K. A. *et al.* Rapid development of a DNA vaccine for Zika virus. *Science* **354**, 237-  
443 240 (2016).  
444 18 Pardi, N., Hogan, M. J., Porter, F. W. & Weissman, D. mRNA vaccines - a new era in  
445 vaccinology. *Nat Rev Drug Discov* **17**, 261-279, doi:10.1038/nrd.2017.243 (2018).  
446 19 Hassett, K. J. *et al.* Optimization of Lipid Nanoparticles for Intramuscular Administration  
447 of mRNA Vaccines. *Mol Ther Nucleic Acids* **15**, 1-11, doi:10.1016/j.omtn.2019.01.013  
448 (2019).  
449 20 Mauger, D. M. *et al.* mRNA structure regulates protein expression through changes in  
450 functional half-life. *Proceedings of the National Academy of Sciences* **116**, 24075,  
451 doi:10.1073/pnas.1908052116 (2019).

- 452 21 Cockrell, A. S. *et al.* A mouse model for MERS coronavirus-induced acute respiratory  
453 distress syndrome. *Nat Microbiol* **2**, 16226-16226, doi:10.1038/nmicrobiol.2016.226  
454 (2016).
- 455 22 Wrapp, D. *et al.* Cryo-EM structure of the 2019-nCoV spike in the prefusion  
456 conformation. *Science* **367**, 1260-1263, doi:10.1126/science.abb2507 (2020).
- 457 23 Freeman, B. *et al.* Validation of a SARS-CoV-2 spike protein ELISA for use in contact  
458 investigations and sero-surveillance. *bioRxiv* (2020).
- 459 24 Klumpp-Thomas, C. *et al.* Standardization of enzyme-linked immunosorbent assays for  
460 serosurveys of the SARS-CoV-2 pandemic using clinical and at-home blood sampling.  
461 *medRxiv*, 2020.2005.2021.20109280, doi:10.1101/2020.05.21.20109280 (2020).
- 462 25 Kim, H. W. *et al.* RESPIRATORY SYNCYTIAL VIRUS DISEASE IN INFANTS DESPITE  
463 PRIOR ADMINISTRATION OF ANTIGENIC INACTIVATED VACCINE12. *American*  
464 *Journal of Epidemiology* **89**, 422-434, doi:10.1093/oxfordjournals.aje.a120955 (1969).
- 465 26 Fulginiti, V. A., Eller, J. J., Downie, A. W. & Kempe, C. H. Altered Reactivity to Measles  
466 Virus: Atypical Measles in Children Previously Immunized With Inactivated Measles  
467 Virus Vaccines. *JAMA* **202**, 1075-1080, doi:10.1001/jama.1967.03130250057008  
468 (1967).
- 469 27 Bolles, M. *et al.* A Double-Inactivated Severe Acute Respiratory Syndrome Coronavirus  
470 Vaccine Provides Incomplete Protection in Mice and Induces Increased Eosinophilic  
471 Proinflammatory Pulmonary Response upon Challenge. *Journal of Virology* **85**, 12201,  
472 doi:10.1128/JVI.06048-11 (2011).
- 473 28 Dinnon, K. H. *et al.* A mouse-adapted SARS-CoV-2 model for the evaluation of COVID-  
474 19 medical countermeasures. *bioRxiv*, 2020.2005.2006.081497,  
475 doi:10.1101/2020.05.06.081497 (2020).
- 476 29 Richner, J. M. *et al.* Modified mRNA Vaccines Protect against Zika Virus Infection. *Cell*  
477 **169**, 176, doi:10.1016/j.cell.2017.03.016 (2017).
- 478 30 ter Meulen, J. *et al.* Human Monoclonal Antibody Combination against SARS  
479 Coronavirus: Synergy and Coverage of Escape Mutants. *PLOS Medicine* **3**, e237,  
480 doi:10.1371/journal.pmed.0030237 (2006).
- 481 31 Douglas, M. G., Kocher, J. F., Scobey, T., Baric, R. S. & Cockrell, A. S. Adaptive  
482 evolution influences the infectious dose of MERS-CoV necessary to achieve severe  
483 respiratory disease. *Virology* **517**, 98-107, doi:10.1016/j.virol.2017.12.006 (2018).
- 484 32 Scobey, T. *et al.* Reverse genetics with a full-length infectious cDNA of the Middle East  
485 respiratory syndrome coronavirus. *Proceedings of the National Academy of Sciences*  
486 **110**, 16157, doi:10.1073/pnas.1311542110 (2013).
- 487 33 Wang, L. *et al.* Evaluation of candidate vaccine approaches for MERS-CoV. *Nature*  
488 *Communications* **6**, 7712, doi:10.1038/ncomms8712 (2015).
- 489 34 Bottcher, E. *et al.* Proteolytic activation of influenza viruses by serine proteases  
490 TMPRSS2 and HAT from human airway epithelium. *J Virol* **80**, 9896-9898,  
491 doi:10.1128/JVI.01118-06 (2006).

492

493

Figure 1



494

495 **Figure 1. MERS-CoV S-2P mRNA protects mice from lethal challenge.** 288/330<sup>+/+</sup> mice were

496 immunized at weeks 0 and 3 with 0.01 (green), 0.1 (blue), or 1  $\mu\text{g}$  (red) of MERS-CoV S-2P

497 mRNA. Mock-immunized mice were immunized with PBS (gray). Two weeks post-boost, sera

498 were collected from 3 mice per group and assessed for neutralizing antibodies against MERS

499 m35c4 pseudovirus (a). Four weeks post-boost, 12 mice per group were challenged with a lethal

500 dose of mouse-adapted MERS-CoV (m35c4). Following challenge, mice were monitored for

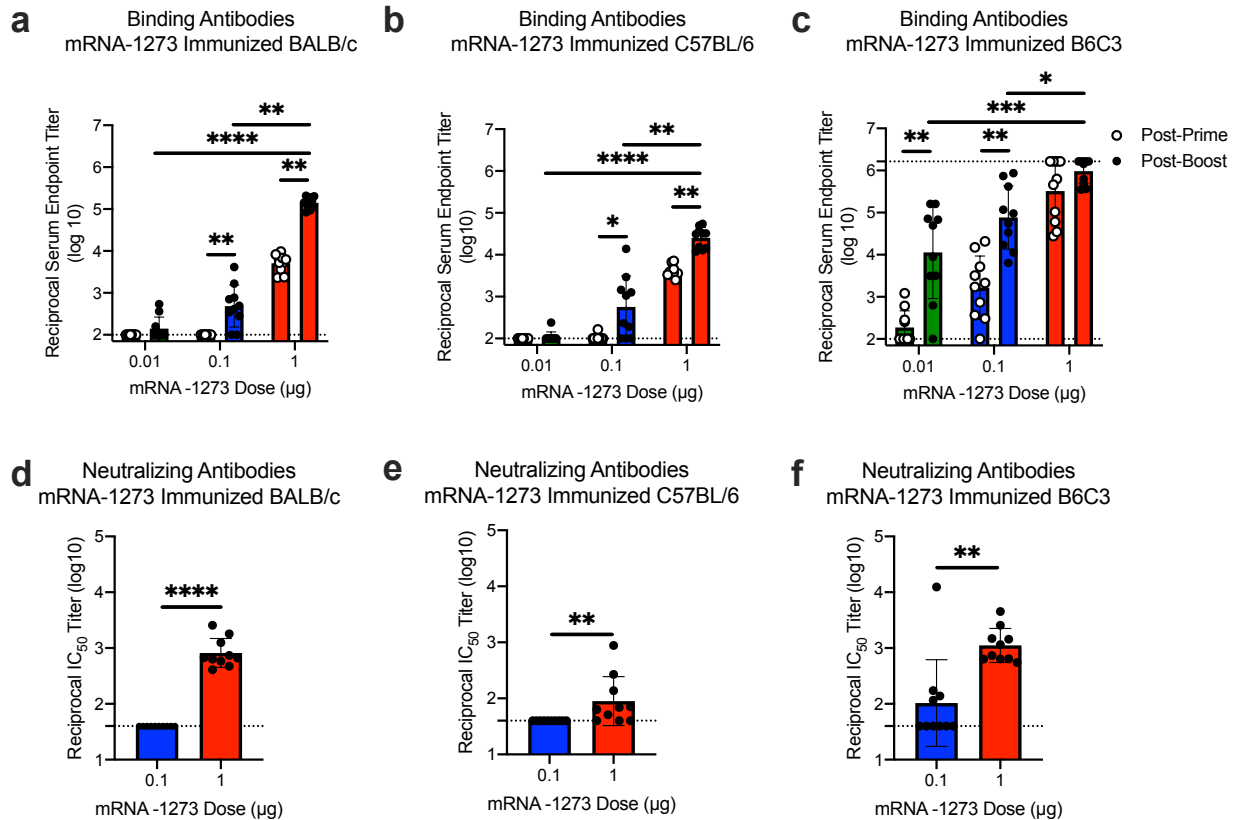
501 weight loss (b). Two days post-challenge, at peak viral load, lung viral titers (c) and hemorrhage

502 (0 = no hemorrhage, 4 = severe hemorrhage in all lobes) (d) were assessed from 5 animals per

## Figure 1

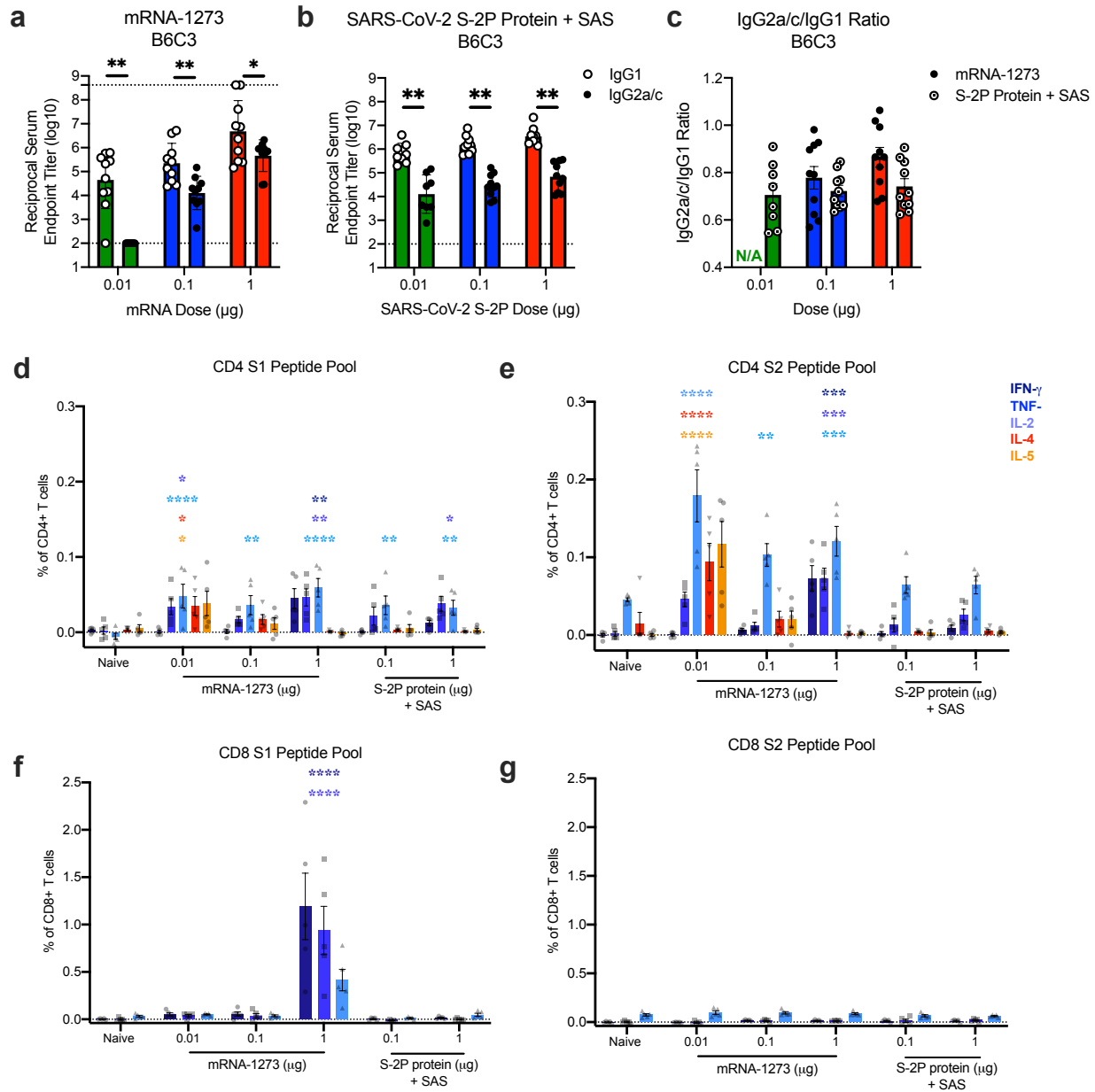
503 group. Dotted line = assay limit of detection. (a, c-d) All dose levels were compared. (b) For  
504 weight loss, all comparisons are against PBS-immunized mice.

Figure 2



**Figure 2.** mRNA-1273 elicits robust binding and neutralizing antibody responses in multiple mouse strains. BALB/cJ (a, d), C57BL/6J (b, e), or B6C3F1/J (c, f) mice were immunized at weeks 0 and 3 weeks with 0.01 (green), 0.1 (blue), or 1 µg (red) of mRNA-1273. Sera were collected 2 weeks post-prime (open circles) and 2 weeks post-boost (closed circles) and assessed for SARS-CoV-2 S-specific IgG by ELISA (a-c), and, for post-boost sera, neutralizing antibodies against homotypic SARS-CoV-2 pseudovirus (d-f). Dotted line = assay limit of detection. (a-c) Timepoints were compared within each dose level, and doses were compared post-boost.

Figure 3



**Figure 3. Immunizations with mRNA-1273 and S-2P protein, delivered with TLR4 agonist, elicit S-specific Th1-biased T cell responses.** B6C3F1/J mice were immunized at weeks 0 and 3 with 0.01, 0.1, or 1 μg of mRNA-1273 or SAS-adjuvanted SARS-CoV-2 S-2P protein. Sera were collected 2 weeks post-boost and assessed by ELISA for SARS-CoV-2 S-specific IgG1 and IgG2a/c. Endpoint titers (a-b) and endpoint titer ratios of IgG2a/c to IgG1 (c) were calculated. For mice for which endpoint titers did not reach the lower limit of detection (dotted line), ratios were



### Figure 3

not calculated (N/A). (d-g) Seven weeks post-boost, splenocytes were isolated from 5 mice per group and re-stimulated with no peptides or pools of overlapping peptides from SARS-CoV-2 S protein in the presence of a protein transport inhibitor cocktail. After 6 hours, intracellular cytokine staining (ICS) was performed to quantify CD4<sup>+</sup> and CD8<sup>+</sup> T cell responses. Cytokine expression in the presence of no peptides was considered background and subtracted from the responses measured from the S1 and S2 peptide pools for each individual mouse. (d-e) CD4<sup>+</sup> T cells expressing IFN- $\gamma$ , TNF $\alpha$ , IL-2, IL-4 and IL-5 in response to the S1 (d) and S2 (e) peptide pools. (f-g) CD8<sup>+</sup> T cells expressing IFN- $\gamma$ , TNF- $\alpha$ , and IL-2 in response to the S1 (f) and S2 (g) peptide pools. IgG1 and IgG2a/c (a-b) and immunogens (c) were compared at each dose level. (d-g) For each cytokine, all comparisons were compared to naïve mice.

Figure 4

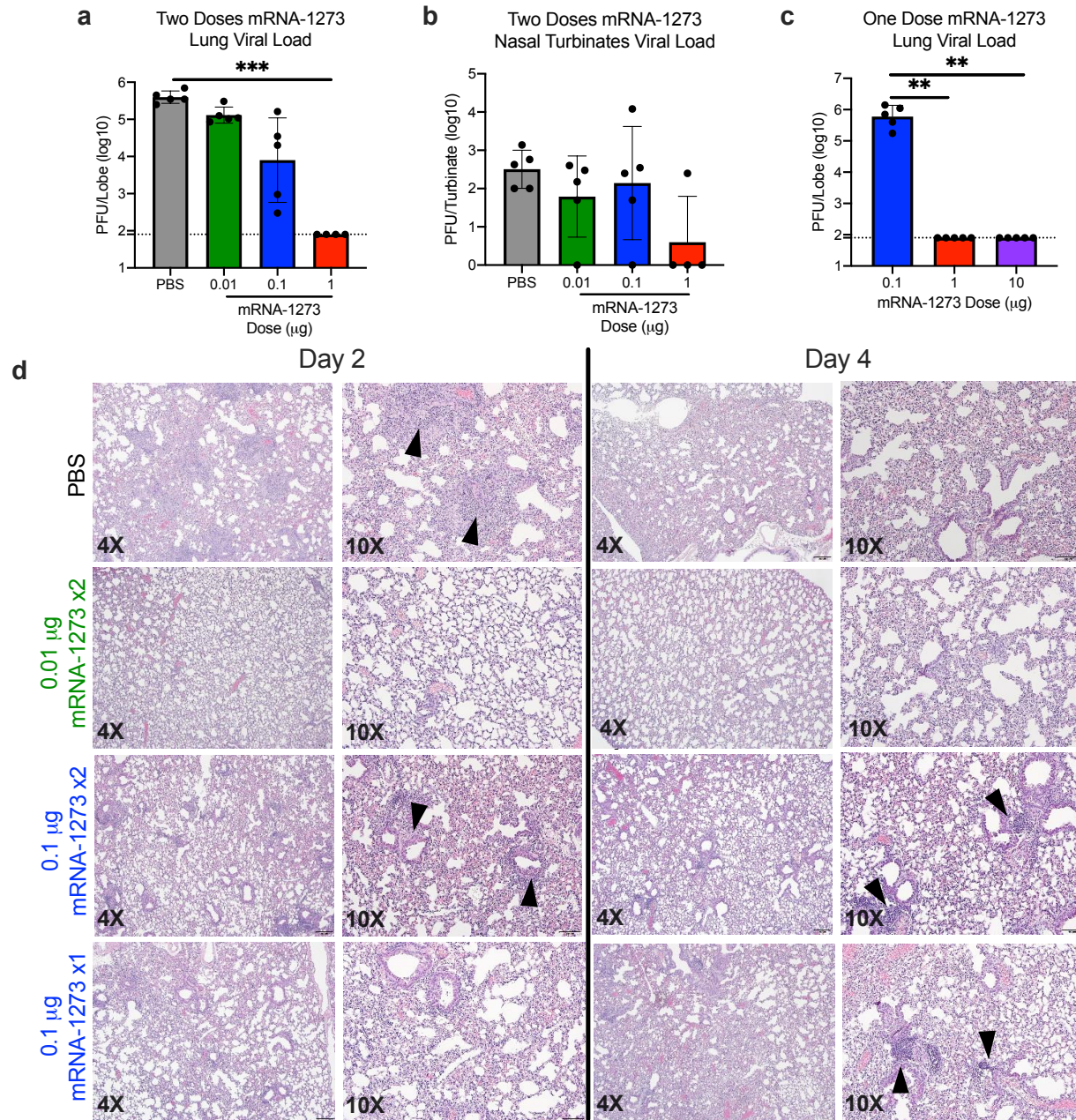


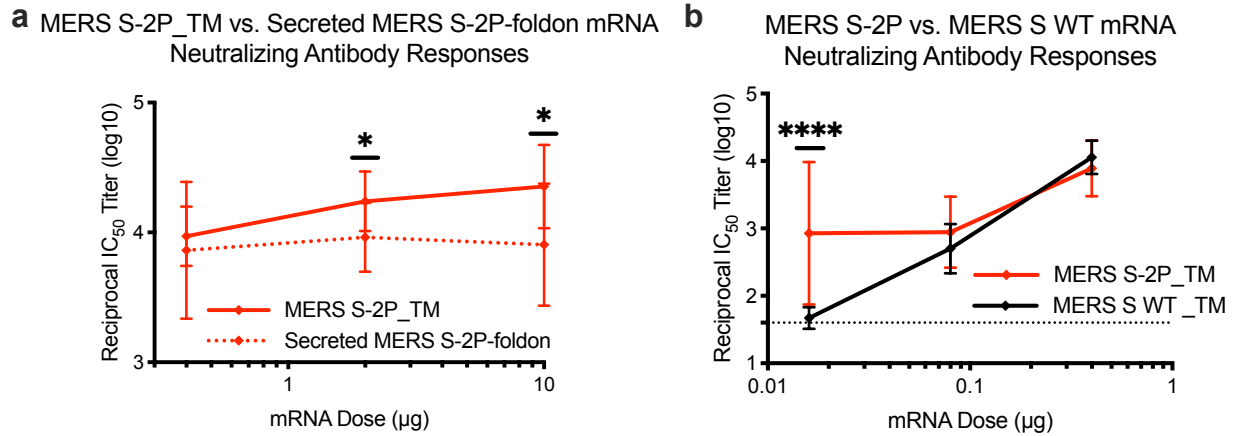
**Figure 4. mRNA-1273 protects mice from upper and lower airway SARS-CoV-2 infection.**

(a-b) BALB/cJ mice were immunized at weeks 0 and 3 with 0.01 (green), 0.1 (blue), or 1  $\mu\text{g}$  (red) of mRNA-1273. Mock-immunized mice were immunized with PBS x2. Five weeks post-boost, mice were challenged with mouse-adapted SARS-CoV-2. (c) BALB/cJ mice were also immunized with a single dose of 0.1 (blue), 1 (red), or 10 (purple)  $\mu\text{g}$  of mRNA-1273 and challenged 7 weeks post-immunization. Two days post-challenge, at peak viral load, mouse lungs (a,c) and nasal

## Figure 4

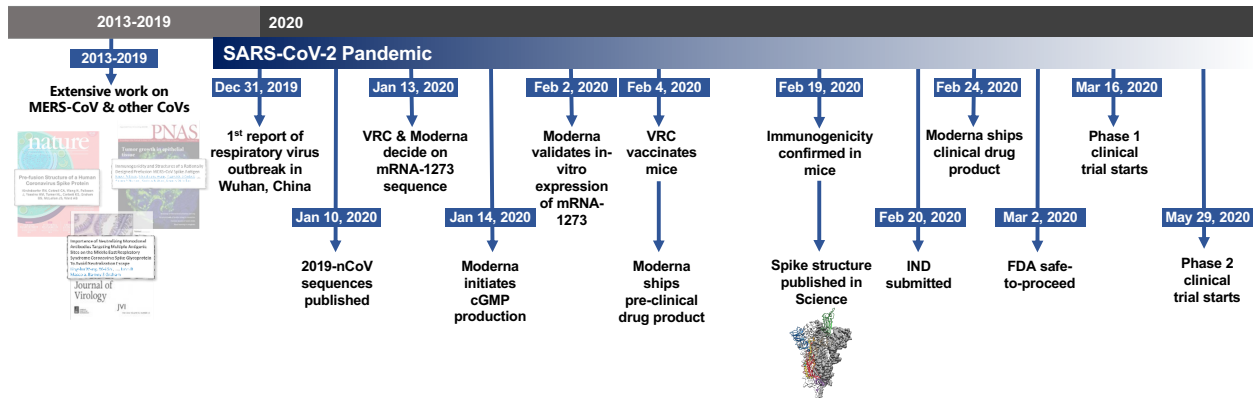
turbinates (b) were harvested from 5 mice group for analysis of viral titers. Dotted line = assay limit of detection. (d) At day 2 and 4 post-challenge, lungs from 5 mice per group were fixed in 10% formalin, paraffin-embedded, cut in 5  $\mu\text{m}$  sections, and stained with hematoxylin and eosin. Photomicrographs (4X and 10X) are representative of lung sections from groups of mice in which virus infection was detected. At day 2, lungs from mock-immunized mice demonstrated moderate to severe, predominantly neutrophilic, inflammation that was present within, and surrounding, small bronchioles (arrowheads); the surrounding alveolar capillaries were markedly expanded by infiltrating inflammatory cells. In the 0.01  $\mu\text{g}$  two-dose group, inflammation was minimal to absent. In the 0.1  $\mu\text{g}$  two-dose group, occasional areas of inflammation intimately associated with small airways (bronchioles) and their adjacent vasculature (arrowheads) were seen, primarily composed of neutrophils. In the single-dose 0.1  $\mu\text{g}$  group, there were mild patchy expansion of the alveolar septae by mononuclear and polymorphonuclear cells. At day 4, lungs from mock-immunized mice exhibited moderate to marked expansion of the alveolar septae (interstitial pattern) with decreased prominence of the adjacent alveolar spaces. In the 0.01  $\mu\text{g}$  two-dose group, inflammation was minimal to absent. Lungs in the 0.1  $\mu\text{g}$  two-dose group showed mild, predominantly lymphocytic inflammation, intimately associated with bronchioles and adjacent vasculature (arrowheads). In the single-dose 0.1  $\mu\text{g}$  group there was mild, predominantly lymphocytic, inflammation around bronchovascular bundles (arrowheads).

## Extended Data Figure 1



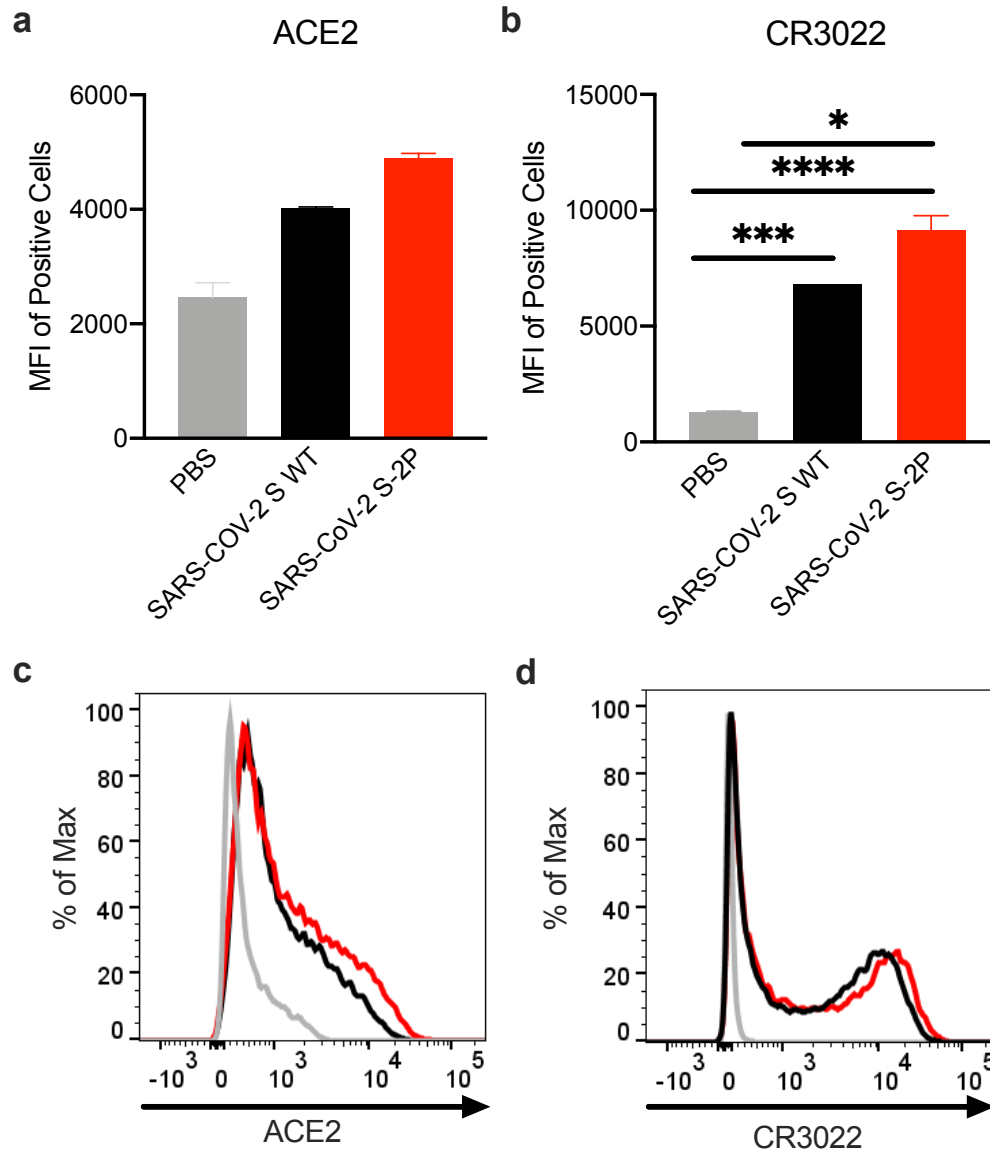
**Extended Data Figure 1. Transmembrane-anchored MERS-CoV S-2P (S-2P\_TM) mRNA elicits more potent neutralizing antibody responses than secreted MERS-CoV S-2P and S WT mRNA.** C57BL/6J mice were immunized at weeks 0 and 4 with (a) 0.4, 2, or 10 µg of MERS-CoV S-2P\_TM (red) or MERS S-2P\_secreted (red hashed) or (b) 0.016 µg, 0.08 µg, or 0.4 µg of MERS-CoV S-2P or MERS-CoV S WT\_TM (black) mRNA. Sera were collected 4 weeks post-boost and assessed for neutralizing antibodies against MERS-CoV m35c4 pseudovirus. Dotted line = assay limit of detection. Immunogens were compared at each dose level

## Extended Data Figure 2



**Extended Data Figure 2. Timeline for mRNA-1273's progression to clinical trial.** The morning after novel coronavirus (nCoV) sequences were released, spike sequences were modified to include prefusion stabilizing mutations and synthesized for protein production, assay development, and vaccine development. Twenty-five days after viral sequences were released, clinically-relevant mRNA-1273 was received to initiate animal experiments. Immunogenicity in mice was confirmed 15 days later. Moderna shipped clinical drug product 41 days after GMP production began, leading to the Phase 1 clinical trial starting 66 days following the release of nCoV sequences.

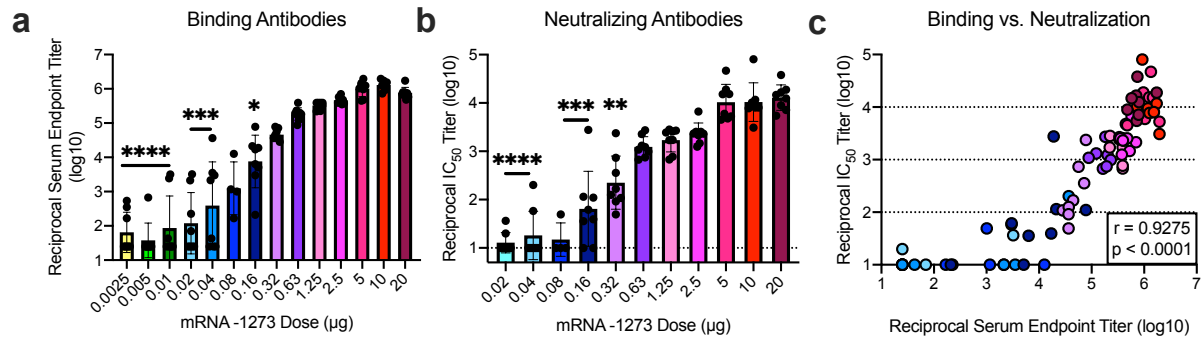
### Extended Data Figure 3



**Extended Data Figure 3. *In vitro* expression of SARS-CoV-2 spike mRNA on cell surface.**

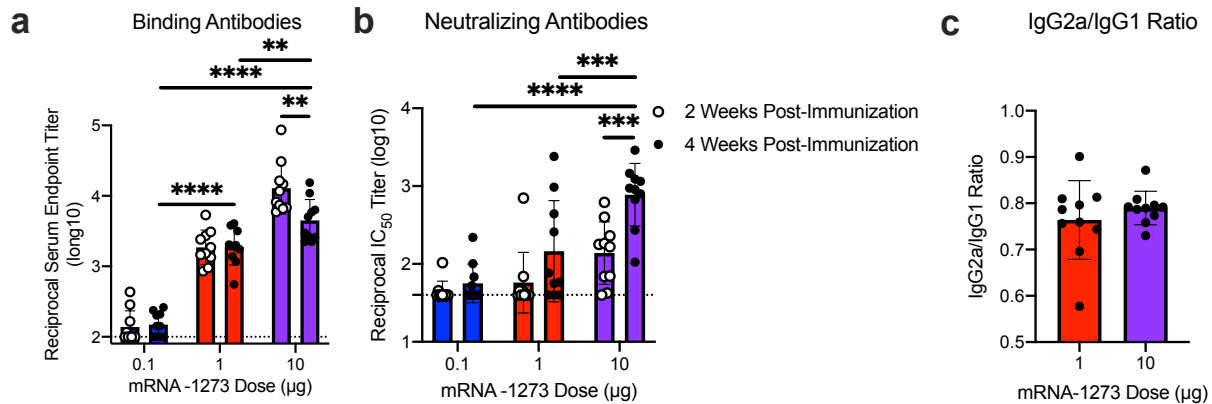
293T cells were transfected with mRNA expressing SARS-CoV-2 wild-type spike (black) or S-2P (red), stained with ACE2 (a,c) or CR3022 (b,d), and evaluated by flow cytometry 24 post-transfection. Mock-transfected (PBS) cells served as a control.

## Extended Data Figure 4



**Extended Data Figure 4. Dose-dependent mRNA-1273-elicited antibody responses reveal strong positive correlation between binding and neutralization titers.** BALB/cJ mice were immunized at weeks 0 and 3 weeks with various doses (0.0025 – 20  $\mu\text{g}$ ) of mRNA-1273. (a-b) Sera were collected 2 weeks post-boost and assessed for SARS-CoV-2 S-specific IgG by ELISA (a) and neutralizing antibodies against homotypic SARS-CoV-2 pseudovirus (b). (a-b) All doses were compared to 20  $\mu\text{g}$  dose.

## Extended Data Figure 5

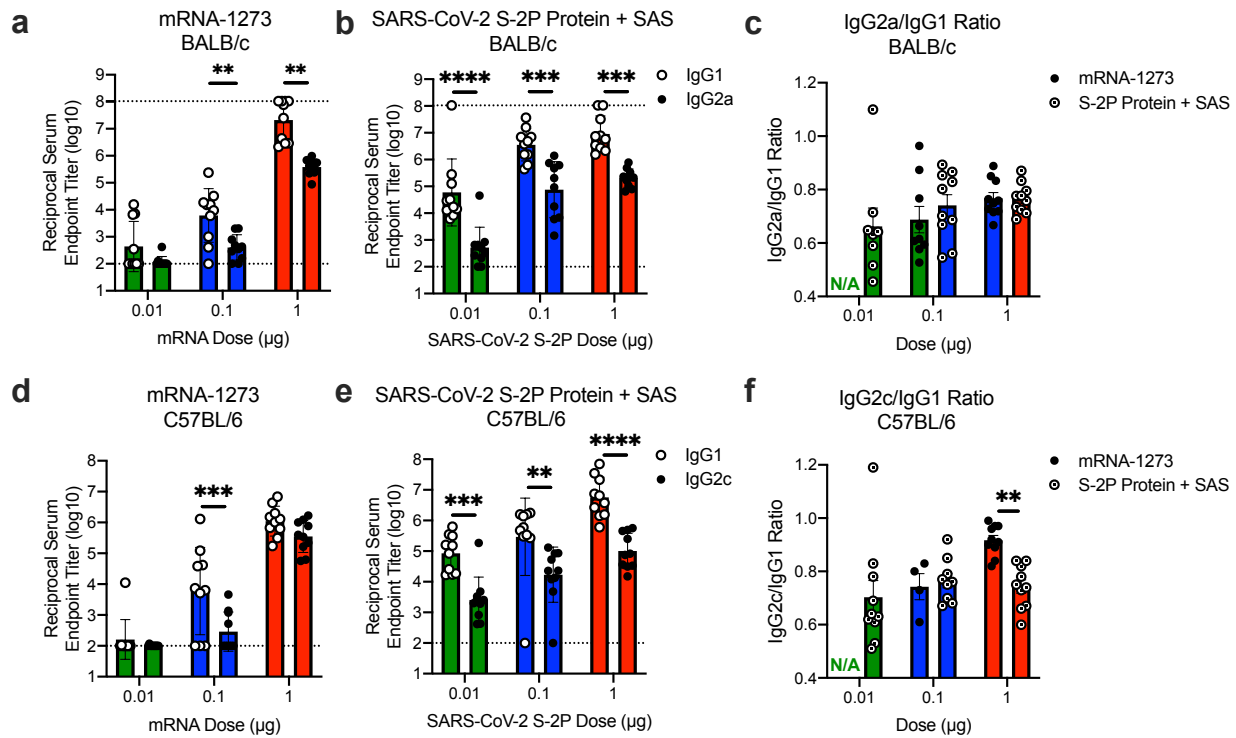


### **Extended Data Figure 5. A single dose of mRNA-1273 elicits robust antibody responses.**

BALB/cJ mice were immunized with 0.1 (blue), 1 µg (red), or 10 µg (purple) of mRNA-1273. Sera were collected 2 (open circles) and 4 (closed circles) weeks post-immunization and assessed for SARS-CoV-2 S-specific total IgG by ELISA (a) and neutralizing antibodies against homotypic SARS-CoV-2 pseudovirus (b). (c) S-specific IgG2a and IgG1 were also measured by ELISA, and IgG2a to IgG1 subclass ratios were calculated. Dotted line = assay limit of detection. (a-b) Doses were compared 4 weeks post-boost, and timepoints were compared within each dose level.

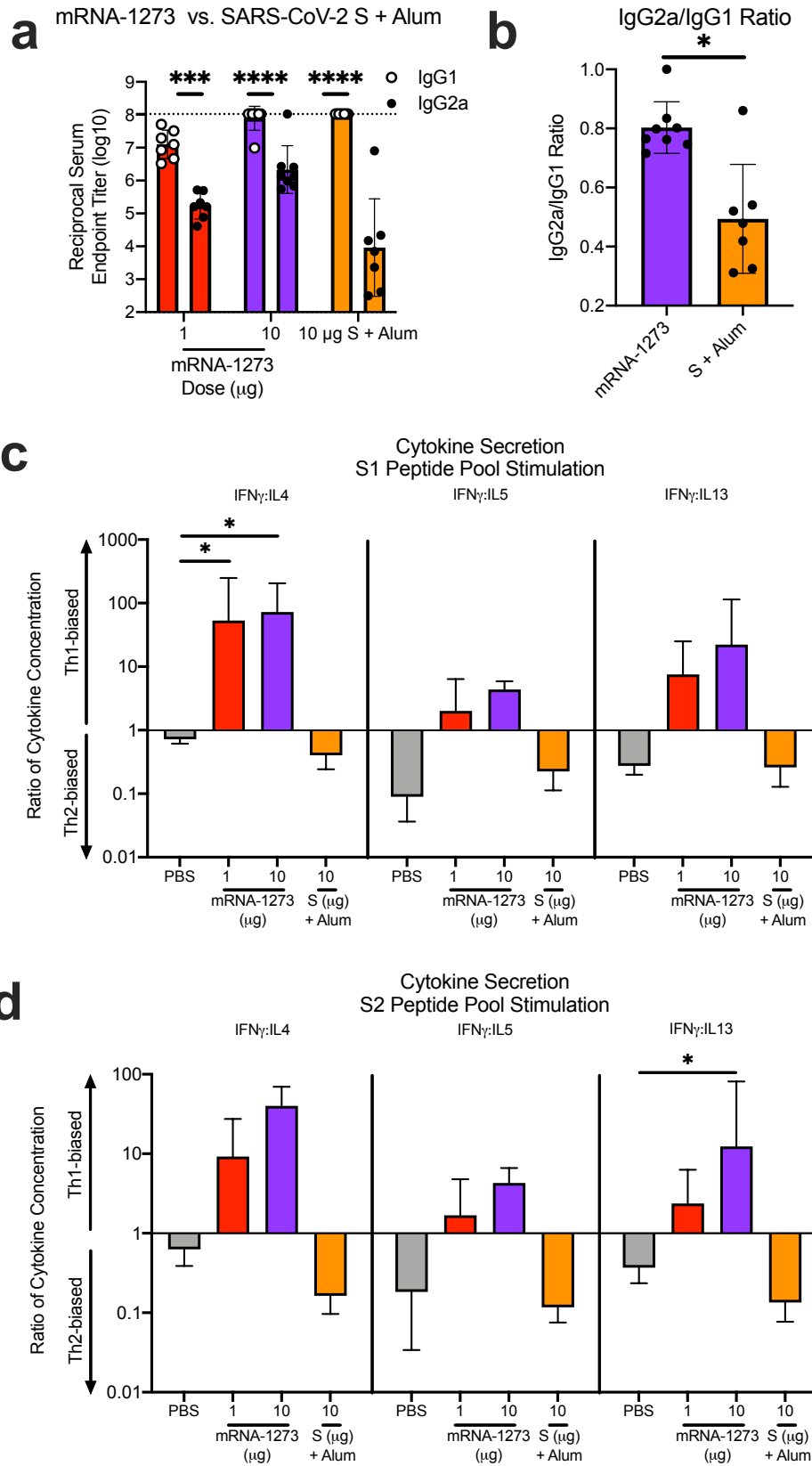


## Extended Data Figure 6



**Extended Data Figure 6. mRNA-1273 and SAS-adjuvanted S-2P protein elicit both IgG2a and IgG1 subclass S-binding antibodies.** BALB/cJ (a-c) or C57BL/6J (d-f) mice were immunized at weeks 0 and 3 with 0.01 (green), 0.1 (blue), or 1  $\mu$ g (red) of mRNA-1273 SARS-CoV-2 S-2P protein adjuvanted with SAS. Sera were collected 2 weeks post-boost and assessed by ELISA for SARS-CoV-2 S-specific IgG1 and IgG2a or IgG2c for BALB/cJ and C57BL/6J mice, respectively. Endpoint titers (a-b, d-e) and endpoint titer ratios of IgG2a to IgG1 (c) and IgG2c to IgG1 (f) were calculated. For mice for which endpoint titers did not reach the lower limit of detection (dotted line), ratios were not calculated (N/A). IgG1 and IgG2a/c (a-b, d-e) and immunogens (c, f) were compared at each dose level.

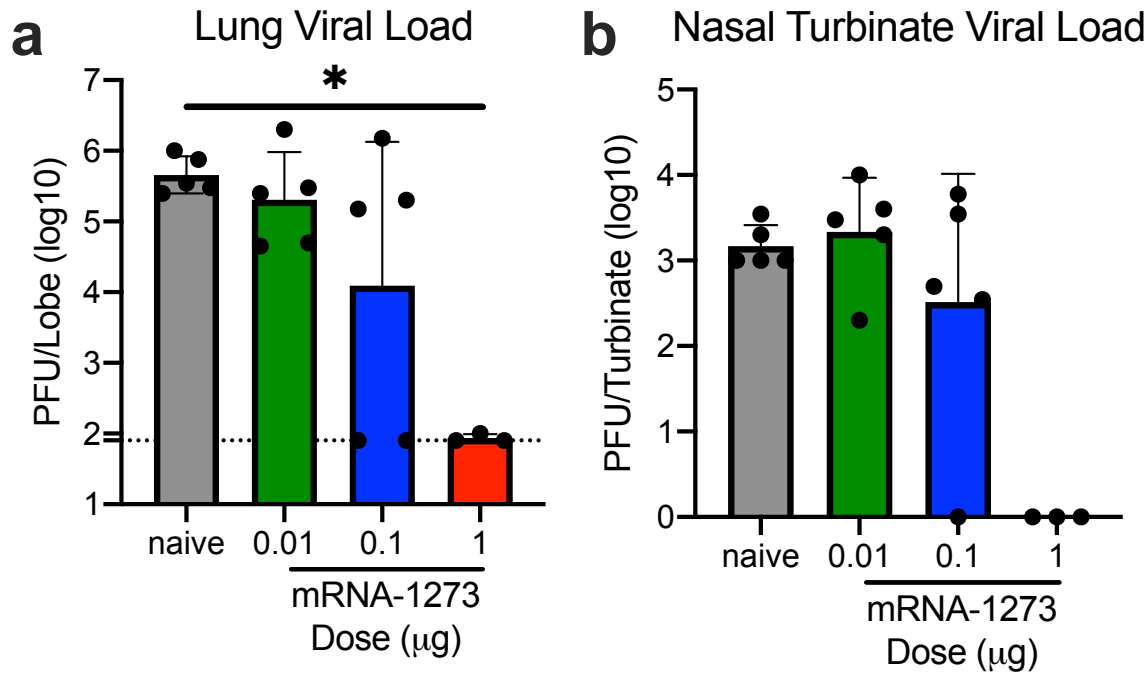
## Extended Data Figure 7



## Extended Data Figure 7

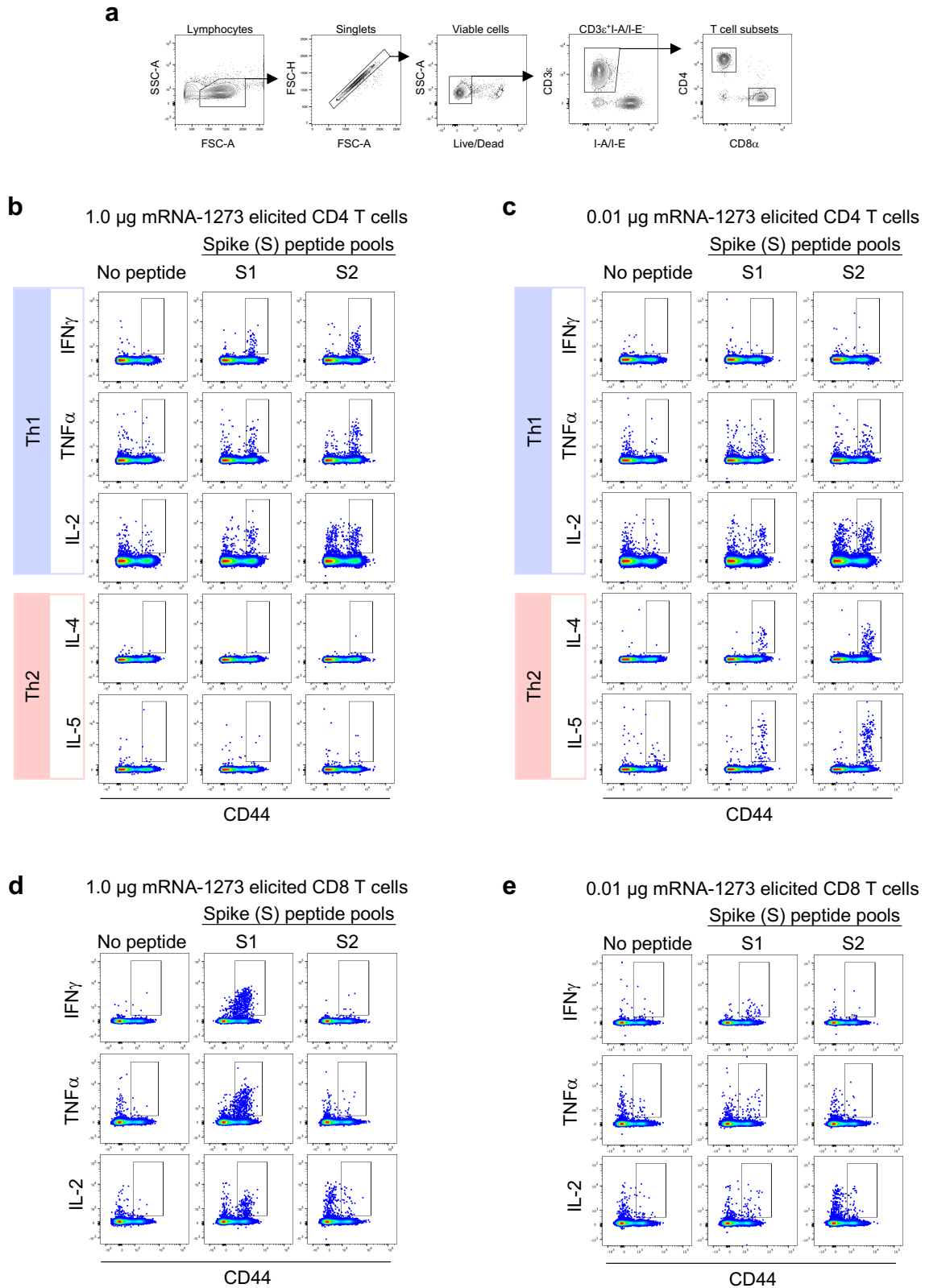
**Extended Data Figure 7. mRNA-1273 elicits Th1-skewed responses compared to S protein adjuvanted with alum.** BALB/c mice were immunized at weeks 0 and 2 weeks with 1 (red) or 10  $\mu\text{g}$  (purple) of mRNA-1273 or 10  $\mu\text{g}$  of SARS-CoV-2 S protein adjuvanted with alum hydrogel (orange). (a-b) Sera were collected 2 weeks post-boost and assessed by ELISA for SARS-CoV-2 S-specific IgG1 and IgG2a. Endpoint titers (a) and endpoint titer ratios of IgG2a to IgG1 (b) were calculated. (c-d) Splenocytes were also collected 4 weeks post-boost to evaluate IFN- $\gamma$ , IL-4, IL-5, and IL-13 cytokine levels secreted by T cells re-stimulated with S1 (c) and S2 (d) peptide pools, measured by Luminex. Dotted line = assay limit of detection. IgG1 and IgG2a/c (a) were compared at each dose level. (c-d) For cytokines, all comparisons were compared to PBS-immunized mice.

## Extended Data Figure 8



**Extended Data Figure 8. mRNA-1273 protects mice from upper and lower airway SARS-CoV-2 infection, 13 weeks post-boost.** BALB/cJ mice were immunized at weeks 0 and 3 with 0.01 (green), 0.1 (blue), or 1  $\mu\text{g}$  (red) of mRNA-1273. Age-matched naive mice (gray) served as controls. Thirteen weeks post-boost, mice were challenged with mouse-adapted SARS-CoV-2. Two days post-challenge, at peak viral load, mouse lungs (a) and nasal turbinates (b) were harvested from 5 mice per group for analysis of viral titers. Dotted line = assay limit of detection. All dose levels were compared.

## Extended Data Figure 9



## Extended Data Figure 9

### **Extended Data Figure 9. Flow cytometry panel to quantify SARS-CoV-2 S-specific T cells**

**in mice.** (a) A hierarchical gating strategy was used to unambiguously identify single, viable

CD4<sup>+</sup> and CD8<sup>+</sup> T cells. Gating summary of SARS-CoV-2 S-specific (b-c) CD4 (b-c) and (d-e)

CD8 (d-e) T cells elicited by 1.0 and 0.01 µg mRNA-1273 immunization. Antigen-specific T cell

responses following peptide pool re-stimulation were defined as CD44<sup>hi</sup>/cytokine<sup>+</sup>.

Concatenated files shown were generated using the same number of randomly selected events

from each animal across the different stimulation conditions using FlowJo software, v1

## Extended Data Figure 9

**Extended Data Table 1. Concordance of Pseudovirus Neutralization Assay and PRNT.**

Mouse Serum Pool # <sup>1</sup>	Reciprocal IC <sub>50</sub> Titer		<i>Fold Difference</i> <sup>4</sup>
	Pseudovirus Neutralization <sup>2</sup>	PRNT <sup>3</sup>	
1	893.5 +/- 1.4	933.5	1.0
2	211.6 +/- 1.5	314.5	0.7
3	159.8 +/- 1.3	397.1	0.5

<sup>1</sup>BALB/cJ mice were immunized at weeks 0 and 3 with 1 µg SARS-CoV-2 S-2P protein, adjuvanted with SAS. Sera were collected 2 weeks post-boost and pooled (N = 3 mice/pool).

<sup>2</sup>IC<sub>50</sub> titers were averaged from pseudovirus neutralization assays completed in 5 experimental replicates. (GMT +/- geometric SD)

<sup>3</sup>IC<sub>50</sub> titer from PRNT assay completed once.

<sup>4</sup>Fold difference calculated as average pseudovirus neutralization IC<sub>50</sub> titer relative to PRNT IC<sub>50</sub> titer.